

# Symmetry-Guaranteed and Accidental Nodal-Line Semimetals in FCC Lattice

Takuto Kawakami and Xiao Hu\*

International Center for Materials Nanoarchitectonics (WPI-MANA),  
National Institute for Materials Science, Tsukuba 305-0044, Japan

(Dated: October 28, 2018)

We demonstrate theoretically that nodal-line semimetal (NLS) states can be realized in face-center-cubic (fcc) lattice with orbits belonging to one irreducible representation, such as  $[p_x, p_y, p_z]$  and/or  $[d_{xy}, d_{xz}, d_{yz}]$ . It is shown that the three orbits are subdivided with respect to the odd- and even-parity upon mirror reflection on high symmetry planes, which yields an analytic expression for the trajectory of NL in momentum space when a tight-binding (TB) model is adopted. It becomes clear that there are two kinds of NLs, a *symmetry-guaranteed* one around the surface of the first Brillouin zone (BZ), and an *accidental* one around the BZ center governed by the hopping integrals. As a realization of the idea, we analyze the fcc photonic crystal composed of dielectric spheres by solving the Maxwell's equations. Two *symmetry-guaranteed* and one *accidental* NLS photonic states are observed. This provides a good platform to confirm experimentally the existence of topological NLS state, and on its own right the topological surface band characterized by the almost flat dispersion is useful for achieving slow light yearned for many applications.

*Introduction.*— Recently, much attention has been paid to nodal-line semimetal (NLS) states, topological semimetals in three dimensions (3D) characterized by energy dispersion with linear band crossing over closed loops in momentum space [1–12]. As the characteristic feature of NLS, a drumhead-shaped surface band appears in the projected surface Brillouin zone (BZ) [1]. Because the density of states is enhanced significantly by this almost-flat band, NLS systems are expected to be ideal platforms for achieving high-temperature superconductors and other novel states with strong correlations [13]. There are a number of theoretical proposals on material realization of NLS states, including perovskite iridates [2, 3], 3D graphene networks [4], antiperovskite materials [5, 6], pnictides [7], metal beryllium [8], and photonic crystal [9]. Several model systems have also been discussed [10–12], and intriguingly NL networks were revealed based on chiral and nonsymmorphic symmetries [12]. To the best of our knowledge, however, the NLS state has yet to be realized experimentally.

In this work, we expose theoretically that in the face-center-cubic (fcc) lattice NLS states can be realized in terms of orbits belonging to one irreducible representation, such as  $[p_x, p_y, p_z]$  and/or  $[d_{xy}, d_{xz}, d_{yz}]$ . It is clarified that, because of the fcc structure, the three orbits are subdivided into the odd- and even-parity upon mirror operation at high symmetry planes. Taking advantage of this property, one can derive an analytic expression for the trajectory of NL in momentum space in the tight-binding (TB) model. It then becomes clear that there are two kinds of NLs, one is guaranteed by the fcc lattice symmetry and appears around the surface of the first BZ, and the other one locates around the BZ center governed by the detailed balance between hopping integrals. Following this guideline, we design a fcc photonic crystal composed of dielectric spheres such as silicon. Solving Maxwell's equations numerically, we

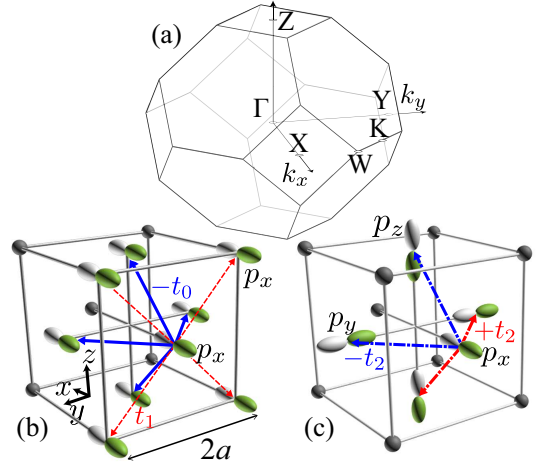


FIG. 1: Schematics for the fcc lattice with  $p$  orbitals residing on lattice sites. (a) First Brillouin zone and symmetric points of the fcc lattice. (b,c) Tight-binding model for three  $p$  orbitals and hoppings between those on the nearest-neighboring sites. Wave functions with positive and negative signs are depicted in gray and green respectively, and positive and negative hopping integrals are indicated in red and blue respectively.

predict two *symmetry-protected* and one *accidental* NLS photonic states. This provides an ideal platform for confirming the NLS state.

*TB model on fcc lattice.*— We consider a fcc lattice with three orbits of one irreducible representation residing on the sites. To be specific, we begin with  $[p_x, p_y, p_z]$ , and for simplicity we concentrate first on TB model with the nearest-neighbor hoppings, noting that the main results remain valid even long-range hoppings are involved. The TB Hamiltonian is given as

$$\hat{H} = \sum_{\alpha, \beta, \mathbf{r}, \mathbf{R}} t^{\alpha\beta}(\mathbf{R}) \hat{c}_{\beta}^{\dagger}(\mathbf{r} + \mathbf{R}) \hat{c}_{\alpha}(\mathbf{r}) \quad (1)$$

where  $\alpha, \beta \in \{x, y, z\}$ ,  $\hat{c}_\alpha(\mathbf{r})$  is the annihilation operator for the  $p_\alpha$  orbit, and the summation is taken over lattice sites  $\mathbf{r}$  and the relative coordinates  $\mathbf{R} = a(\pm\hat{y} \pm \hat{z})$ ,  $a(\pm\hat{z} \pm \hat{x})$  and  $a(\pm\hat{x} \pm \hat{y})$  for the nearest neighbors in the fcc lattice, with  $\hat{x}$  the unit vector in the  $x$  axis and so on for the other two directions, and  $a$  half of the length of simple cubic [see Figs. 1(b) and (c)].

The fcc lattice structure puts the following constraints on the hopping integrals: (i) as read from Fig. 1(b), the hopping integrals between the same orbits are given as

$$t^{\alpha\alpha}(\mathbf{R}) = \begin{cases} t_1, & \text{for } \mathbf{R} \perp \hat{\alpha}, \\ -t_0, & \text{otherwise} \end{cases} \quad (2)$$

with  $t_0$  and  $t_1$  positive; (ii) as read from Fig. 1(c), hoppings between different orbits  $p_\alpha$  and  $p_\beta$  are allowed only in the  $\alpha\beta$ -plane with the hopping integrals given by

$$t^{\alpha\beta}(\mathbf{R}) = \begin{cases} \pm\epsilon_{\alpha\beta}t_2, & \text{for } \mathbf{R} \parallel \hat{\alpha} \pm \hat{\beta}, \\ 0, & \text{otherwise} \end{cases} \quad (3)$$

where  $t_2 > 0$ ,  $\epsilon_{xy} = \epsilon_{yz} = \epsilon_{zx} = 1$  and antisymmetric upon permutation.

The Fourier transformation of Hamiltonian (1) with Eqs. (2) and (3) gives the Bloch Hamiltonian  $H(\mathbf{k})$  with the matrix elements

$$H_{\alpha\alpha}(\mathbf{k}) = -4t_0 \cos(k_\alpha a) \sum_{\beta \neq \alpha} \cos(k_\beta a) + 4t_1 \prod_{\beta \neq \alpha} \cos(k_\beta a), \quad (4)$$

$$H_{\alpha\beta}(\mathbf{k}) = -4t_2 \sin(k_\alpha a) \sin(k_\beta a). \quad (5)$$

The first BZ of the fcc lattice is shown in Fig. 1(a).

Of many symmetries inherent in the fcc lattice, mirror symmetry is crucial for achieving the NLS state [14]. To be specific, we consider the mirror operation with respect to  $xy$ -plane. The mirror symmetry of the present system is characterized by  $\mathcal{M}_{xy}H(k_x, k_y, -k_z)\mathcal{M}_{xy}^{-1} = H(k_x, k_y, k_z)$ . On the  $k_z = 0$  plane, where the commutation relation  $[\mathcal{M}_{xy}, H(\mathbf{k})] = 0$  is satisfied, the Hamiltonian is block diagonalized according to the eigenvalues of  $\mathcal{M}_{xy}$ ,  $m_{xy} = \pm 1$ , the parity upon the mirror reflection. It is obvious that  $p_x$  and  $p_y$  orbits fall into the even-parity block while  $p_z$  orbit in the odd-parity block. Therefore, on the  $k_z = 0$  plane  $p_x$  and  $p_y$  orbits do not interact with  $p_z$  orbit, a feature forbidding gap opening at band crossing.

Taking advantage of this mirror symmetry we can analytically diagonalize the Bloch Hamiltonian (4, 5) (see supplement [15]), and derive an analytic expression for the trajectory of NL, where the energies of different parity states are degenerate. On the  $k_z = 0$  plane, the NL should obey

$$(1 - 4\tau^2) \cos(k_x a) \cos(k_y a) + \cos(k_x a) + \cos(k_y a) + 1 = 0 \quad (6)$$

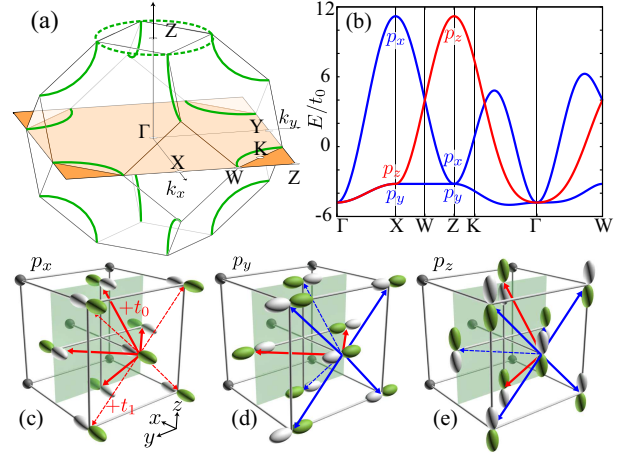


FIG. 2: (a) Distributions of NLs (green curves) in the first BZ in fcc lattice with three  $p$  orbitals. (b) Dispersion relations along several momentum directions, where the red curve is for the band with large weight of  $p_z$  orbit. Parameters are  $t_1 = 0.8t_0$  and  $t_2 = 1.2t_0$  satisfying  $\tau < 1$ . (c-e) Hopping integrals between orbits at the X-points.

with  $\tau \equiv (t_0 + t_1)/2t_2$  [15]. It is obvious that, independently of hopping integrals, Eq. (6) is satisfied at  $W$  point  $(k_x a, k_y a) = (\pm\pi, \pm\pi/2), (\pm\pi/2, \pm\pi)$ , and hence a NL including  $W$  point always exists as *guaranteed* by symmetry [see Fig. 1(a)]. On the other hand, at  $\Gamma$  point the left hand side of Eq. (6) changes sign at  $\tau = 1$ , indicating that there is an *accidental* NL at the zone center when the coupling integrals satisfy  $\tau > 1$ .

First we focus on the regime  $\tau < 1$ , with the NLs shown in Fig. 2(a) in accordance to Eq. (6) and its counterparts in the other two mirror symmetric planes. Dispersions at several typical cuts in momentum space of  $k_z = 0$  are displayed in Fig. 2(b). Linear band crossings are clearly observed at  $W$  point and a point between  $K$  and  $\Gamma$  points inside the BZ. In terms of the reciprocal lattice vectors of the fcc lattices, they form a closed loop at  $k_z = \pi/a$  as depicted by the dashed line in Fig. 2(a).

In order to examine the origin of band crossing, let us pay attention to the energies of the three  $p$  orbitals at  $X$  point  $\mathbf{k} = \pi a^{-1}\hat{x}$ . It is clear that the wave functions on planes of  $x = (2n+1)a$  get  $\pi$  phase as shown in Figs. 2(c-e), and thus all the hopping integrals between  $p_x$  orbitals become positive, in contrast with those in Fig. 1(b) for  $\Gamma$  point, which contribute to energy coherently. On the other hand,  $p_y$ - $p_y$  and  $p_z$ - $p_z$  hopping integrals still take opposite signs in different directions, which results in cancellations in contributions to energy. Furthermore,  $p_x$ - $p_y$  and  $p_x$ - $p_z$  hoppings do not contribute to energy due to symmetry as read from Fig. 1(c). As the result, the  $p_x$  orbit carries the highest energy at  $X$  point. Similarly, at  $Y$  and  $Z$  points,  $p_y$  and  $p_z$  orbitals carry the highest energy respectively. Therefore, inversion between energy levels of the  $p_x$  ( $p_y$ ) and  $p_z$  bands should take place between

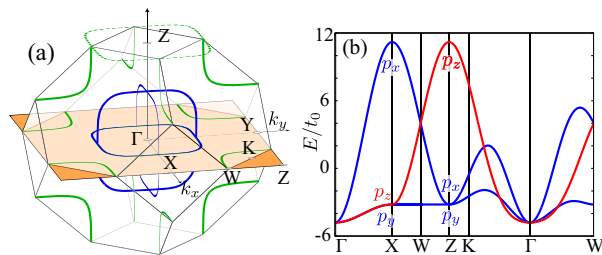


FIG. 3: Same for Fig. 2 except for  $t_2 = 0.5t_0$  satisfying  $\tau > 1$  where *accidental* NLs appear around  $\Gamma$  point in addition to the *symmetry-guaranteed* ones.

$X$  ( $Y$ ) and  $Z$  points, as seen in Fig. 2(a). The Dirac-like dispersion without gap opening is in accordance with the mirror symmetry discussed above.

For  $\tau > 1$ , in addition to the NLs close to the surface of BZ, there appear NLs surrounding  $\Gamma$  point as shown in Fig. 3(a). Band crossings can be seen in dispersion relations as shown in Fig. 3(b). The shape of NLs, both *symmetry-guaranteed* and *accidental*, changes with values of hopping integrals, and they become straight lines and touch with each other for  $\tau \gg 1$  (for details see supplementary materials [15]).

It is worth noticing that the cubic symmetry of fcc crystal guarantees the band inversions around the zone boundary in the present system. For example, the band inversion between  $p_x$  and  $p_z$  orbits at the NLs between  $X$  and  $Z$  points [see Figs. 2(a) and (b) and 3] is supported by invariance of the system under  $\pi/2$  rotation around the  $y$ -axis. Therefore, the existence of the *symmetry-guaranteed* NL is universal beyond the TB model discussed above. It is then not difficult to find that the three  $d$  orbits can also be exploited for achieving the NL by means of the same mechanism, since the three orbits are subdivided into two in the odd-parity sector and one in the even-parity sector with respect to the mirror reflection, and the rotation symmetry around the three main axes is the same as that for  $p$  orbits.

*Photonic NLS state.* — As a realistic system exhibiting NLs based on the mechanism discussed above, we consider a fcc photonic crystal of dielectric spheres such as silicon. It is well known that in metamaterials, where ions in materials are replaced by a periodic arrangement of permittivity and/or permeability, frequency dispersions and band structures of electromagnetic modes appear as the result of Bloch theorem [16]. It also became clear that topological states can be realized in photonic systems quite similarly to electronic materials [17–19]. In the present system, Maxwell’s equations for the harmonic modes of electromagnetic waves with  $\mathbf{E}(\mathbf{r}, t) = \mathbf{E}(\mathbf{r}) \exp(i\omega t)$  and  $\mathbf{B}(\mathbf{r}, t) = \mathbf{B}(\mathbf{r}) \exp(i\omega t)$  are

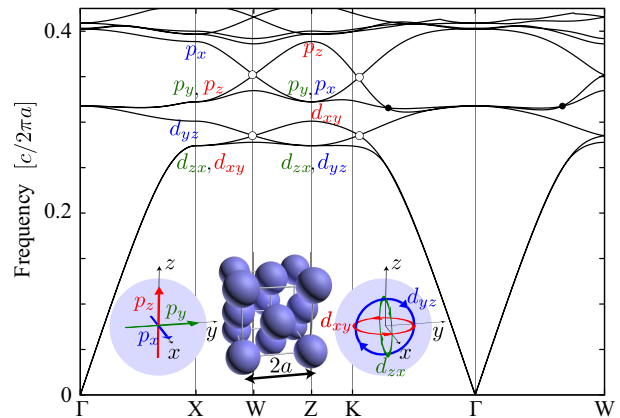


FIG. 4: Band dispersion of a fcc lattice of dielectric spheres shown in the central inset, where there are two sets of *symmetry-guaranteed* (denoted by open circles) and one set of *accidental* (denoted by dots) NLs. Distributions of electric field at the center of spheres are displayed schematically for the  $p$  and  $d$  orbits in the left and right insets respectively (for details see the text). The radius of spheres is  $R = 0.5a$  and the relative permittivity is  $\epsilon_{\text{fcc}} = 11.56$ .

simplified into [16]

$$\frac{1}{\epsilon(\mathbf{r})} \nabla \times \nabla \times \mathbf{E}(\mathbf{r}) = \frac{\omega^2}{c^2} \mathbf{E}(\mathbf{r}) \quad (7)$$

for the electric field, and the magnetic field is given by the Faraday relation  $\mathbf{H} = -i/(\mu_0\omega) \nabla \times \mathbf{E}$ , where  $\epsilon(\mathbf{r})$  is the position-dependent relative permittivity and  $c = 1/\sqrt{\epsilon_0\mu_0}$  is the light velocity in vacuum. Equation (7) can be solved numerically in momentum space using the package MIT PHOTONIC BANDS [20], and the dispersion relations of an infinite system are displayed in Fig. 4(a) along the same momentum directions given in Fig. 2(a). It is clear that there are three sets of Dirac-like band crossing at  $\omega/\omega_0 \simeq 0.29$ ,  $\simeq 0.32$  and  $\simeq 0.35$  with  $\omega_0 = 2\pi a/c$ .

Let us first focus on the high-frequency NLS state. Upon the spatial inversion the electric field is mapped by  $\mathbf{E}(\mathbf{r}) \rightarrow -\mathbf{E}(-\mathbf{r})$ , and thus  $\mathbf{E}(\mathbf{r}) = \pm \mathbf{E}(-\mathbf{r})$  for odd- and even-parity states respectively. On the other hand, upon the mirror reflection with respect to the  $yz$  plane, the electric field is mapped by  $\mathbf{E}(\mathbf{r}) \rightarrow \mathcal{M}_{yz}(\mathbf{E}(\mathcal{M}_{yz}(\mathbf{r}))) \equiv [-E_x(-x, y, z), E_y(-x, y, z), E_z(-x, y, z)]$ , and two other corresponding relations for the  $xy$  and  $xz$  planes, and one has  $\mathbf{E}(\mathbf{r}) = \pm \mathcal{M}_{\alpha\beta}(\mathbf{E}(\mathcal{M}_{\alpha\beta}(\mathbf{r})))$  for even- and odd-parity states respectively. Checking the wave function of the electric field upon these two symmetry operations, we find that the orbit at  $X$  point with frequency  $\omega/\omega_0 \simeq 0.39$  exhibits the symmetry same as  $p_x$  orbit. There are two degenerate modes at  $X$  point with frequency  $\omega/\omega_0 \simeq 0.32$ , which are identified in the same way as  $p_y$ - and  $p_z$ -like orbits. Along the  $XW$  direction, the energy of  $p_x$ -like ( $p_z$ -like) mode decreases (increases) and meet at  $W$  point to form the Dirac-like energy dispersion at  $\omega/\omega_0 \simeq 0.35$ .

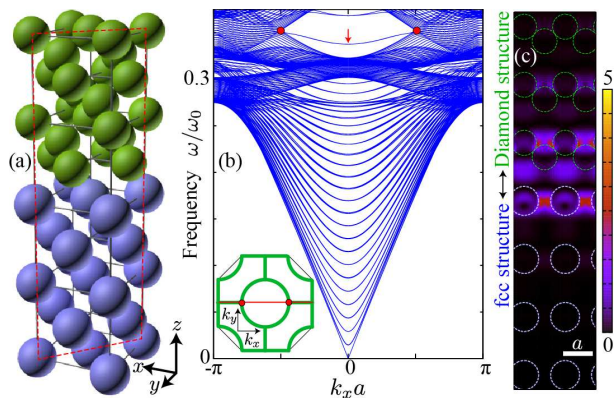


FIG. 5: (a) Heterostructure of the fcc and diamond lattices with the same lattice constant. (b) Band dispersion for  $k_y = 0$  of the structure shown in (a), with the projected BZ and NLs in  $k_x$ - $k_y$  plane displayed in the inset. (c) Intensity of the electric field in arbitrary unit on the cross section of the heterostructure indicated by dashed line in (a) for the almost-flat band at  $\Gamma$  point. The thickness of the fcc (diamond) lattice is of  $34a$  ( $16a$ ), and the permittivity of spheres in the diamond lattice is  $\epsilon_{\text{dia}} = 5.78$ . All other parameters are the same as those in Fig. 4.

Therefore, the NLS state around  $\omega/\omega_0 \simeq 0.35$  is well described by the TB model, even though electromagnetic waves distribute over the whole space in between the dielectric spheres. This indicates clearly that the NLS state is governed by the symmetry, and the picture derived based on the TB model with nearest-neighbor hoppings holds for broad classes of physical systems.

As the topological feature of a NLS state, 2D states characteristic of almost-flat dispersions appear at the interface between the NLS and a trivial insulating system[1]. Because the vacuum does not behave as an insulator for photons, one needs to prepare a topologically trivial photonic insulator to realize the interface. It is known that there is a global photonic gap in the diamond lattice of dielectric spheres [21]. The BZs of the fcc and diamond lattices are equivalent to each other when the same cubic size is taken, since the diamond lattice consists of the fcc Bravais lattice with two dielectric spheres in the primary unit cell. Adopting dielectric spheres in the diamond lattice with half of the permittivity of those in the fcc lattice, one can tune the photonic gap of the diamond lattice to the frequency of the NLS state in the fcc lattice (for details see supplementary materials [15]). For silicon in the fcc lattice, we can choose the lead glass for the diamond lattice [22]. In order to examine the interfacial mode, we consider the super lattice structure shown in Fig. 5(a). For a slab infinite in the  $xy$  plane, momenta  $k_x$  and  $k_y$  are good quantum number, and thus the projected NLs displayed in the inset of Fig. 5(b) are expected. The numerical results obtained by solving the Maxwell equation (7) are displayed in Fig. 5(b), where an almost flat band can be observed, which generates elec-

tromagnetic waves with very small group velocity. As shown in Fig. 5(c), the flat-band mode is well localized the interface between the fcc and diamond lattices. It is noticed that, within the projected NL loop around  $\Gamma$  point indicated in the inset of Fig. 5(b), all the states are gapped except for the almost-flat band, indicating that this surface state is stable.

In the same way, we find that the NLS state around  $\omega/\omega_0 \sim 0.29$  in Fig. 4 is achieved by  $d$  orbits. Interface states similar to that shown in Fig. 5 are also realized in this case. The  $p$  and  $d$  bands appear in frequency bands well separated from each other close to the surface of BZ, and therefore can be treated independently for discussion on the *symmetry-guaranteed* NLS. In contrary, there is an *accidental* NL around  $\Gamma$  point at  $\omega/\omega_0 \simeq 0.32$ , where one cannot identify clearly the orbits as  $p$  or  $d$ , and therefore the NL is supported merely by the mirror symmetry. At  $\Gamma$  point, the triplet at  $\omega/\omega_0 \simeq 0.32$  is of  $d$  orbits whereas that at  $\omega/\omega_0 \simeq 0.4$  is of  $p$  orbits, corresponding to the  $T_{2g}$  and  $T_{1u}$  representations of the  $O_h$  point group.

*Discussions.*— While the signs in hopping integral do not affect the existence of the *symmetry-guaranteed* NLS, they increase the group velocities around the nodal points in terms of the energy difference between the orbits at the high symmetry points. This property is not only helpful for observing the NL itself, but also ideal for applications since it generates a large energy gap around the interface states surrounded by the NLs as seen in Fig. 5(b). Since the topological interface band is almost flat in momentum space, the group velocity is extremely small, which can be used for achieving slow light yearned for many applications [23].

The mechanism yielding *symmetry-guaranteed* NL discussed so far does not apply for the simple cubic (SC) and body centered cubic (BCC) lattices. For SC lattice, the reciprocal lattice vectors in momentum space never translate  $Z$  point to the  $k_z = 0$  plane. One might think the energy degeneracy supported by the fourfold rotation symmetry of SC lattice useful. However, the two orbits degenerate upon rotation around the  $z$  axis are  $p_x$  and  $p_y$  orbits, which exhibits the same parity upon mirror reflection with respect to the  $k_z = 0$  plane and thus will open an energy gap when the two orbits meet. On the other hand, for BCC lattice,  $X$ ,  $Y$  and  $Z$  points are equivalent, called  $H$  point, in terms of the reciprocal lattice vectors. Therefore, the three  $p$  (or  $d$ ) orbits are all degenerate at the same points, which cannot guarantee band crossing.

*Conclusions.*— We discover a new mechanism for realizing nodal-line semimetal states in fcc lattice with three  $p$  (and/or  $d$ ) orbits residing on the sites, taking advantage of the mirror and rotational symmetries. It becomes clear that in this system there are two kinds of nodal line, *symmetry-guaranteed* and *accidental* with the latter gov-

erned by values of hopping integrals. We propose the fcc photonic crystal composed of dielectric spheres, and predict that there are two *symmetry-guaranteed* and one *accidental* nodal-line photonic states. This provides a good platform to confirm experimentally the existence of topological nodal-line semimetal state.

*Acknowledgements.*— This work was supported by the WPI Initiative on Materials Nanoarchitectonics, Ministry of Education, Culture, Sports, Science and Technology of Japan, and Grants-in-Aid for Scientific Research (No.16K17755), JSPS.

---

\* Correspondence to: HU.Xiao@nims.go.jp

- [1] A. A. Burkov, M. D. Hook, and L. Balents, Phys. Rev. B **84**, 235126 (2011).
- [2] Y. Chen, Y.-M. Lu, and H.-Y. Kee, Nat. Commun. **6**, 6593 (2015).
- [3] H.-S. Kim, Y. Chen, and H.-Y. Kee, Phys. Rev. B **91**, 235103 (2015).
- [4] H.-M. Weng, Y. Liang, Q. Xu, R. Yu, Z. Fang, X. Dai, and Y. Kawazoe, Phys. Rev. B **92**, 045108 (2015).
- [5] Y. Kim, B. J. Wieder, C. L. Kane, and A. M. Rappe, Phys. Rev. Lett. **115**, 036806 (2015).
- [6] R. Yu, H. Weng, Z. Fang, X. Dai, and X. Hu, Phys. Rev. Lett. **115**, 036807 (2015).
- [7] A. Yamakage, Y. Yamakawa, Y. Tanaka, and Y. Okamoto, J. Phys. Soc. Jpn. **85**, 013708 (2016).
- [8] R. Li, H. Ma, X. Cheng, S. Wang, D. Li, Z. Zhang, Y. Li, and X.-Q. Chen, Phys. Rev. Lett. **117**, 096401 (2016).
- [9] L. Lu, L. Fu, J. D. Joannopoulos, and M. Soljačić, Nature Photonics **7**, 294 (2013).
- [10] K. Mullen, B. Uchoa, and D. T. Glatzhofer, Phys. Rev. Lett. **115**, 026403 (2015).
- [11] M. Ezawa, Phys. Rev. Lett. **116**, 127202 (2016).
- [12] T. Bzdusek, Q.-S. Wu, A. Rüegg, M. Sigrist, A. A. Soluyanov, Nature **538**, 75 (2016).
- [13] N. B. Kopnin, T. T. Heikkilä and G. E. Volovik, Phys. Rev. B **83**, 220503 (2011).
- [14] C.-K. Chiu and A. P. Schnyder, Phys. Rev. B **90** 205136 (2014).
- [15] See Supplemental Material
- [16] J. D. Joannopoulos, S. G. Johnson, J. N. Winn, and R. D. Meade, Photonic Crystals: Molding the Flow of Light, 2nd ed. (Princeton University Press, New Jersey, 2008).
- [17] F.D.M.Haldane, and S. Raghu, Phys. Rev. Lett. **100**, 013904 (2008).
- [18] L.-H. Wu and X. Hu, Phys. Rev. Lett. **114**, 223901 (2015).
- [19] L. Lu, J. D. Joannopoulos, and M. Soljačić, Nat. Phys., **12**, 626 (2016).
- [20] S. G. Johnson and J. D. Joannopoulos, Opt. Express **8**, 173 (2001).
- [21] K. M. Ho, C. T. Chan, and C. M. Soukoulis, Phys. Rev. Lett. **65**, 3152 (1990).
- [22] K. Umahankar, Introduction to Engineering Electromagnetic Fields (World Scientific Publishing, Singapore, 1989).
- [23] T. F. Krauss, Nat. Photon. **2**, 448 (2008).